J. Chem. Eng. Data **1997,** *42,* 1269−1273 **1269**

Vapor−Liquid Equilibrium, Coexistence Curve, and Critical Locus for Difluoromethane + Pentafluoroethane (R-32 + R-125)

Yukihiro Higashi

Department of Mechanical Engineering, Iwaki Meisei University, 5-5-1, Iino, Chuodai, Iwaki 970, Japan

The vapor−liquid equilibrium for difluoromethane + pentafluoroethane (R-32 + R-125) was measured by the static method in the temperature range between 283 K and 313 K. The vapor−liquid coexistence curve near the critical point was measured by the observation of the meniscus disappearance. The critical temperatures and critical densities of a 30 mass % R-32 and a 60 mass % R-32 mixture were determined on the basis of the saturation densities along the coexistence curve in the critical region. In addition, the critical locus for the R-32 + R-125 mixture is correlated as the function of composition.

Introduction

Because of their low ozone-depleting potentials, hydrofluorocarbon (HFC) mixtures are expected to be considered as alternative refrigerants for R-22 as the working fluid of refrigerator and heat pump systems. However, reliable information on the thermophysical properties of these mixtures is very restricted, and it is difficult for many researchers of HFC mixtures to obtain the highest performance of their machinery.

This paper reports equilibrium measurements of the most promising binary mixtures, that is, difluoromethane (CH_2F_2; R-32) and pentafluoroethane (C_2HF_5; R-125) mixtures. The first measurement is that of the vapor−liquid equilibrium, and the second is that of the vapor−liquid coexistence curve near the critical point.

Experimental Section

Chemicals. The samples of pure R-32 and pure R-125 were furnished by Asahi Glass Co. Ltd. The manufacturer stated that the sample purities were 99.98 mass % R-32 and 99.99 mass % R-125. These samples were used without further purification.

Apparatus for Vapor−Liquid Equilibrium Measurements. The measurements of the vapor−liquid equilibrium were carried out by the static method (Higashi, 1995). A schematic diagram of the apparatus is shown in Figure 1. The vapor−liquid equilibrium cell (A) is a cylindrical pressure vessel made of 304 stainless steel without a glass window. The inner volume of this cell is about 150 cm^3, and inner height is about 3 cm. This cell was especially designed to minimize the inner height of the cell in order to avoid gradients of concentration occurring due to the gravity near the critical point. This cell is immersed in the thermostated water bath (B), which is kept at a constant temperature (± 5 mK) using a PID controller (F) and two electric heaters (300 W and 1500 W). The cylinder for the liquid phase (J) and that for the vapor phase (K) are connected with the vapor−liquid equilibrium cell. These cylinders have inner volumes of 75 cm^3 and were used as the sampling vessels. Compositions of the vapor phase and the liquid phase for the mixtures were determined with a gas chromatograph (Shimadzu GC-7AG) equipped with a thermal conductivity detector. With respect to this mixture, a Porapak-Q column (2m long, i.d. 3 mm, mesh range 50/80) was used. This gas chromatograph was calibrated with pure components of known purity and with mixtures of known composition that were prepared gravimetrically. The uncertainty of the composition measurements is estimated to be within ±0.4 mol %.

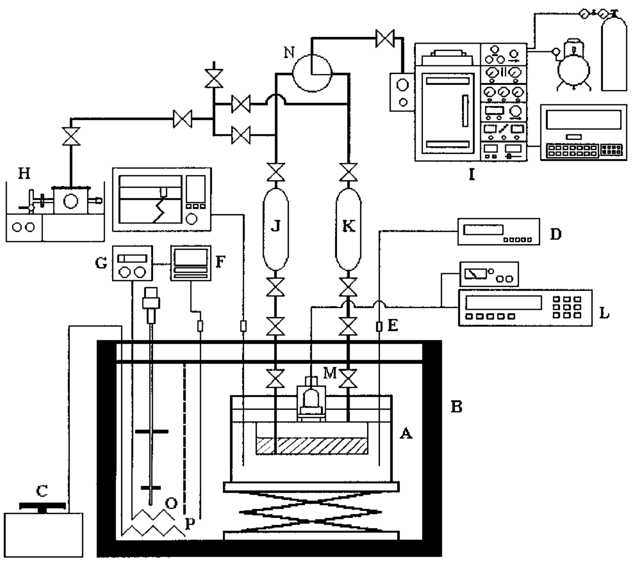

Figure 1. Experimental apparatus for vapor−liquid equilibrium measurements: (A) vapor−liquid equilibrium cell; (B) thermostated bath; (C) voltage converter; (D) thermometer bridge; (E) 100 Ω platinum resistance thermometer; (F) PID controller, (G) thyristor regulator; (H) vacuum pump; (I) gas chromatograph; (J) cylinder for liquid sampling; (K) cylinder for vapor sampling; (L) digital multimeter; (M) pressure transducer; (N) three-way valve; (O) 300 W heater; (P) 1500 W heater.

Temperatures were measured with a 100 Ω platinum resistance thermometer (Automatic Systems Laboratories, F250). This thermometer was calibrated against ITS-90 using a 25 Ω standard platinum resistance thermometer. The uncertainty of temperature measurements is estimated to be within ±10 mK.

The pressure of the sample was measured with a diaphragm semiconductor strain gauge pressure transducer (M) installed in the equilibrium cell. This pressure transducer was calibrated against another quartz crystal pressure transducer (Paroscientific, 2900AT) after every series of experiments. The uncertainty of the pressure measurements is estimated to be within ±0.4%.

Apparatus for the Vapor−Liquid Coexistence Curve Measurement. The measurements of the vapor−liquid coexistence curve near the critical point were carried out on the basis of the observation of the meniscus disappear-

S0021-9568(97)00108-8 CCC: $14.00

Table 1. Vapor−Liquid Equilibrium Data of the R-32 (A) + R-125 (B) Mixture

T/K	P/kPa	x_A	y_A
283.05	905.$_8$	0.0000	0.0000
283.05	992.$_3$	0.241$_4$	0.283$_8$
283.05	1058.$_8$	0.457$_0$	0.500$_1$
283.05	1102.$_6$	0.710$_0$	0.735$_3$
283.05	1125.$_2$	0.895$_0$	0.897$_4$
283.05	1104.$_7$	1.0000	1.0000
293.05	1202.$_1$	0.0000	0.0000
293.05	1310.$_3$	0.241$_5$	0.279$_3$
293.05	1395.$_3$	0.453$_6$	0.493$_2$
293.05	1456.$_8$	0.709$_6$	0.732$_9$
293.05	1480.$_0$	0.896$_0$	0.897$_5$
293.10	1472.$_2$	1.0000	1.0000
303.04	1563.$_8$	0.0000	0.0000
303.04	1700.$_6$	0.235$_7$	0.266$_6$
303.04	1801.$_5$	0.448$_3$	0.487$_3$
303.04	1894.$_1$	0.708$_6$	0.728$_7$
303.04	1923.$_9$	0.895$_9$	0.896$_5$
302.99	1922.$_4$	1.0000	1.0000
313.03	2001.$_5$	0.0000	0.0000
313.04	2167.$_6$	0.225$_0$	0.257$_0$
313.04	2306.$_9$	0.448$_8$	0.478$_3$
313.06	2477.$_7$	1.0000	1.0000

ance. The author has already described in detail the experimental apparatus in the previous paper (Higashi, 1994).

The main portion of the apparatus is composed of an optical cell, an expansion vessel, and a supply vessel. The optical cell is the main vessel in which the change of the meniscus behavior of the sample mixture is observed. The cylindrical body of this optical cell was made of 304 stainless steel (50 mm long, 16−18 mm inner diameter, and 12 cm^3 inner volume) with two Pyrex windows (15 mm in thickness). The inner shape of this optical cell is barrel-shaped in order to make it easier to observe the meniscus disappearance. The expansion vessel and supplying vessel are used to change the sample density in the optical cell without new sample charge.

The apparatus was installed in a thermostated silicone oil bath. The bath temperature can be kept constant within a temperature fluctuation of ±5 mK. Temperature measurement was made with a 25 Ω standard platinum resistance thermometer calibrated against ITS-90 with the aid of a thermometer bridge thermometer (Automatic Systems Laboratories, F17A). The thermometer was mounted in the vicinity of the optical cell. The uncertainty of temperature measurements was estimated to be within ±10 mK.

For the preparation of the sample mixture with a prescribed density and composition, additional pressure vessels were used to fill each of them with the respective compositions. These vessels were filled with the appropriate components and weighed on a precision chemical balance with an uncertainty of 2 mg. Whenever any overestimation of the mass of components was found, the component fluid had to be discharged to the necessary extent. Then each component was transferred successively to the supplying vessel that had been evacuated in advance up to around 0.5 mPa and well cooled by the liquefied nitrogen. It was estimated that the uncertainty of the mass of the sample thus obtained was not greater than 0.1%. In addition, the uncertainty of the composition of the sample was estimated to be within ± 0.05%. In this experiment, a gas chromatograph is not used to determine the composition.

Experimental Results

Vapor−Liquid Equilibrium. The experimental results for the vapor−liquid equilibria (VLE) for R-32 + R-125 are given in Table 1. Measurements were made along four isotherms, e.g., (283.05, 293.05, 303.04, and 313.04) K, and the vapor pressure for each pure component was determined. For the vapor pressures of pure components, the comparison between the present data and the correlation by Piao (1997) for R-32 is shown in Figure 2, whereas that by Piao and Noguchi (1996) for R-125 is shown in Figure 3. The present data are in good agreement with Piao's correlation in the deviation between −0.08% and +0.15% for R-32 and within ±0.04% for R-125, respectively.

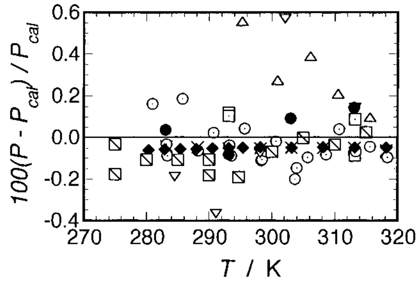

Figure 2. Comparison of the vapor pressure for R-32 between the experimental data and the correlation by Piao (1997): (●) present work; (▽) Malbrunot et al. (1968); (△) Holcomb et al. (1993); (⊡) Bouchot and Richon (1994); (×) Defibaugh et al. (1994); (⊙) Polonara (1994); (slashed □) Widiatmo et al. (1994); (◆) De Vries (1996).

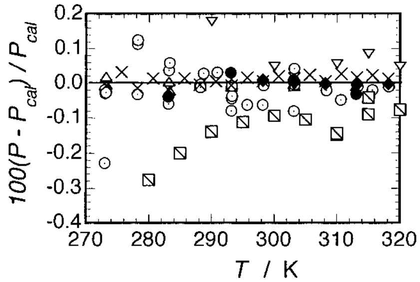

Figure 3. Comparison of the vapor pressure for R-125 between the experimental data and the correlation by Piao and Noguchi (1996): (●) present work; (⊙) Polonara (1994); (slashed □) Widiatmo et al. (1994); (▽) Ye et al. (1994); (×) Boyes and Weber (1995); (△) Gorenflo (1996); (◆) De Vries (1996).

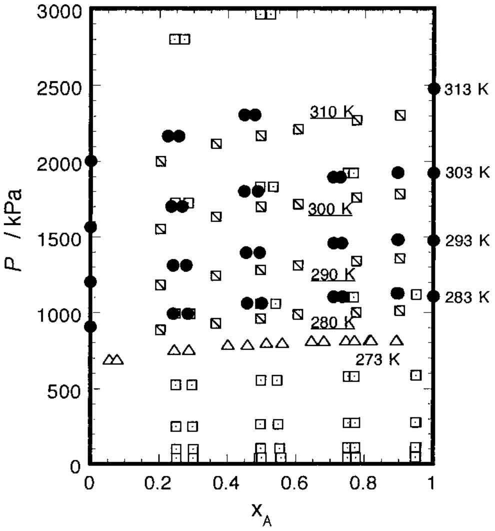

Figure 4. Vapor−liquid equilibria of the R-32(A) + R-125(B) mixture on the pressure−composition diagram: (●) present work; (△) Fujiwara et al. (1992); (slashed □) Widiatmo et al. (1994); (⊡) Nagel and Bier (1995).

Experimental results for the vapor−liquid equilibrium for R-32 + R-125 have been published by Fujiwara et al.

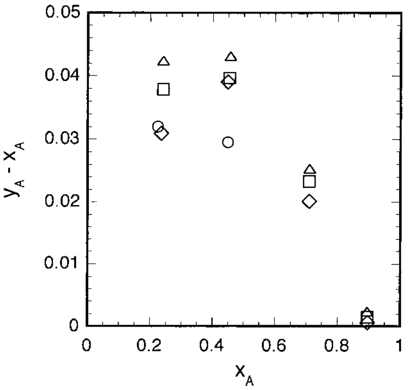

Figure 5. Plot of the difference between vapor composition and liquid composition ($y_A - x_A$) against liquid composition x_A for R-32 (A) + R-125 (B): (△) 283.05 K; (□) 293.05 K; (◇) 303.04 K; (○) 313.04 K.

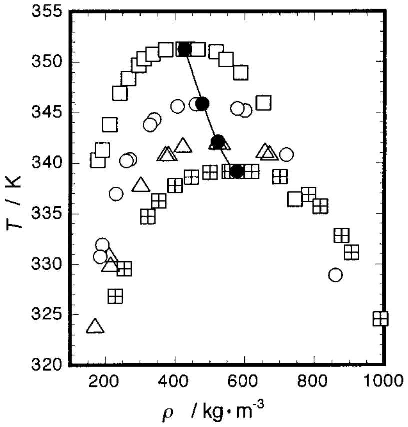

Figure 6. Vapor−liquid coexistence curve of the R-32 (A) + R-125 (B) mixture in the critical region: (□ with a plus) R-125; (△) 30.00 mass % R-32; (○) 60.00 mass % R-32; (□) R-32; (●) critical point; (—) Critical locus.

Table 2. Experimental Data of the Vapor−Liquid Coexistence Curve for the R-32 + R-125 Mixture near the Critical Point

30.00 mass % R−32		60.00 mass % R−32	
T/K	ρ/kg·m^{-3}	T/K	ρ/kg·$^{-3}$ m^{-3}
340.98	671.0 ± 0.7	340.81	719.1 ± 0.7
341.22	657.9 ± 0.7	345.18	600.9 ± 0.6
342.06	532.4 ± 0.9	345.37	578.8 ± 0.6
342.09	522.0 ± 0.9	345.81	476.8 ± 0.9
341.79	422.4 ± 1.3	345.80	475.2 ± 0.5
340.91	380.1 ± 1.2	345.78	459.2 ± 0.8
340.92	372.7 ± 1.2	345.59	407.3 ± 1.3
337.93	301.7 ± 1.2	344.28	340.5 ± 1.1
330.03	215.5 ± 1.2	343.78	327.9 ± 1.1
323.93	171.0 ± 1.1	340.22	260.2 ± 1.0
		336.93	230.8 ± 1.2
		331.93	193.0 ± 1.0
		330.77	185.9 ± 1.0

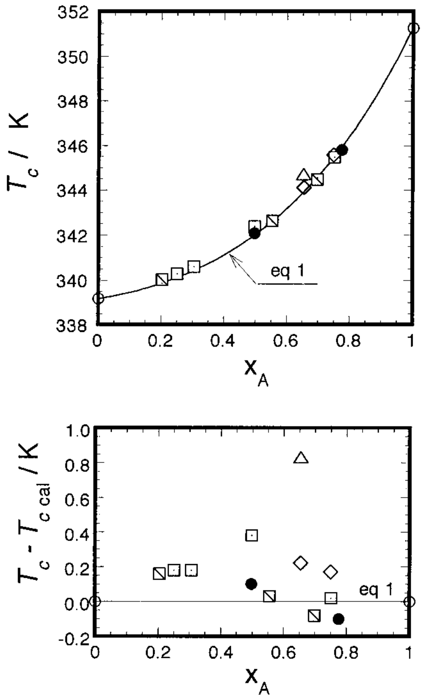

Figure 7. Comparison of the critical temperature of the R-32 (A) + R-125 (B) mixture between the experimental data and eq 1: (●) present work; (○) Higashi (1994); (◇) Zhelezny et al. (1995); (△) Bivens et al. (1995); (⊡) Nagel and Bier (1995); (slashed □) Kishizawa et al. (1997).

Table 3. Critical Parameters of the R-32 (A) + R-125 (B) Mixture

w_A	x_A	T_c/K	ρ_c/kg·m^{-3}	V_c/cm^3·mol^{-1}
0	0	339.17 ± 0.01	577 ± 5	208 ± 2
0.3000	0.4972	342.09 ± 0.02	523 ± 3	165 ± 1
0.6000	0.7758	345.81 ± 0.02	478 ± 4	141 ± 1
1	1	351.26 ± 0.01	427 ± 5	122 ± 2

Table 4. Critical Parameter Table for the R-32 (A) + R-125 (B) Mixture

w_A	x_A	T_c/K	V_c/ cm^3·mol^{-1}	ρ_c/ kg·m^{-3}	P_c/ kPa
0.0000	0.0000	339.17	208.0	577.0	3620
0.0500	0.1083	339.48	199.0	566.2	3782
0.1000	0.2040	339.87	190.8	556.3	3936
0.1500	0.2893	340.33	183.4	547.1	4083
0.2000	0.3658	340.84	176.7	538.4	4222
0.2500	0.4347	341.40	170.6	530.1	4354
0.3000	0.4972	341.99	165.1	522.2	4481
0.3500	0.5540	342.60	160.0	514.5	4602
0.4000	0.6060	343.24	155.4	507.1	4717
0.4500	0.6537	343.89	151.2	499.9	4827
0.5000	0.6976	344.56	147.3	492.8	4933
0.5500	0.7382	345.23	143.7	485.8	5034
0.6000	0.7758	345.91	140.4	479.0	5131
0.6500	0.8108	346.59	137.4	472.2	5224
0.7000	0.8433	347.27	134.6	465.5	5314
0.7500	0.8738	347.94	132.1	458.9	5400
0.8000	0.9022	348.62	129.7	452.4	5482
0.8500	0.9289	349.29	127.5	446.0	5562
0.9000	0.9541	349.95	125.4	439.6	5639
0.9500	0.9777	350.61	123.6	433.3	5713
1.0000	1.0000	351.26	121.8	427.0	5785

(1992), Widiatmo et al. (1993), and Nagel and Bier (1995). The distributions of VLE results for the R-32 + R-125 mixture are shown in Figure 4 on a pressure−composition diagram. In addition, the plot of the difference between vapor composition y_A and liquid composition x_A, that is ($y_A - x_A$), against liquid composition x_A is shown in Figure 5 in order to check the thermodynamic consistency. On the basis of Figures 4 and 5, it was confirmed this R-32 + R-125 mixture had an azeotrope at the composition near 90 mol % R-32. This azeotropic composition is almost independent of temperature.

Vapor−Liquid Coexistence Curve near the Critical Point. The vapor−liquid coexistence curves near the critical point for the 30 mass % R-32 + 70 mass % R-125 mixture and 60 mass % R-32 + 40 mass % R-125 mixture were measured by the observation of meniscus disappearance. The experimental data obtained are given in Table 2 and shown in Figure 6 on the temperature−density plane. The experimental results of pure components reported by the author (Higashi, 1994) are also shown in Figure 6. The full circle denotes the critical point deter-

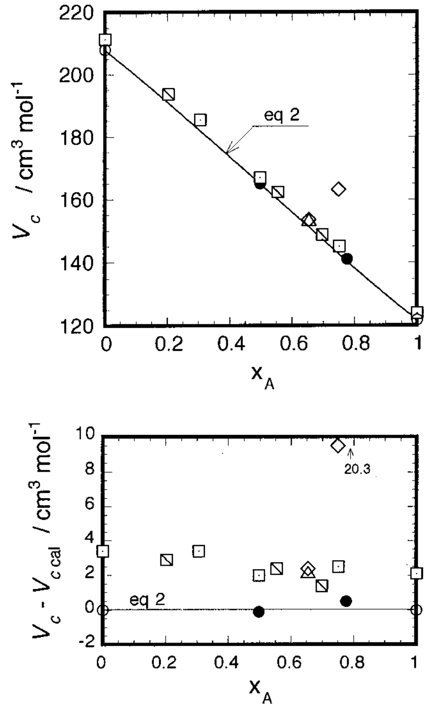

Figure 8. Comparison of the critical molar volume of the R-32 (A) + R-125 (B) mixture between the experimental data and eq 2: (●) present work; (○) Higashi (1994); (◇) Zhelezny et al. (1995); (△) Bivens et al. (1995); (⊡) Nagel and Bier (1995); (slashed □) Kishizawa et al. (1997).

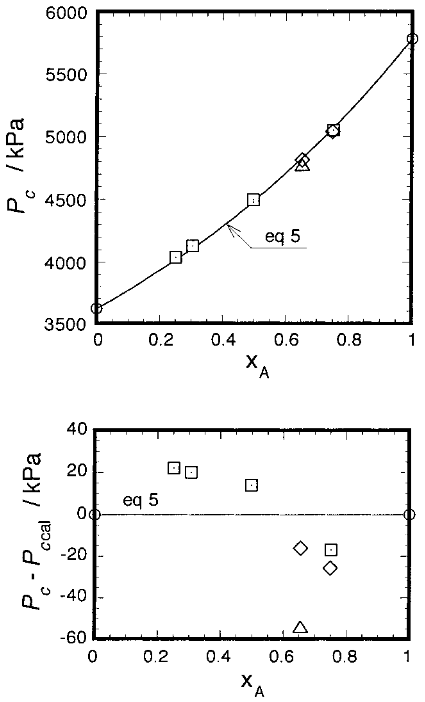

Figure 9. Comparison of the critical pressure of the R-32 (A) + R-125 (B) mixture between the experimental data and eq 5: (○) Higashi (1994); (◇) Zhelezny et al. (1995); (△) Bivens et al. (1995); (⊡) Nagel and Bier (1995).

mined taking into consideration the meniscus disappearing level as well as the intensity of the critical opalescence. The solid line in Figure 6 indicates the critical locus for the R-32 + R-125 mixture. The critical temperature T_c, critical density ρ_c, and critical molar volume V_c of this mixture are summarized in Table 3.

Discussion

Correlation of the Critical Locus. To represent the composition dependence of the critical parameters of mixture, the correlation of the critical locus is formulated. The functional forms of this correlation are as follows (Higashi, 1986, Higashi et al., 1988):

$$T_{cm} = \theta_1 T_{c1} + \theta_2 T_{c2} + 2\theta_1\theta_2\Delta_T \tag{1}$$

$$V_{cm} = \theta_1 V_{c1} + \theta_2 V_{c2} + 2\theta_1\theta_2\Delta_V \tag{2}$$

$$\rho_{cm} = M/V_{cm} \tag{3}$$

$$\theta_i = \frac{x_i V_{ci}^{2/3}}{\sum_j x_j V_{cj}^{2/3}} \tag{4}$$

$$P_{cm} = \theta_1 P_{c1} + \theta_2 P_{c2} + 2\theta_1\theta_2\Delta_P \tag{5}$$

Here T_{cm}, V_{cm}, ρ_{cm}, and P_{cm} denote the critical temperature of mixture, the critical molar volume of mixture, the critical density of mixture, and the critical pressure of mixture, respectively. The surface fraction θ_i defined by eq 4 was adopted. Δ_T in eq 1, Δ_V in eq 2, and Δ_P in eq 5 are the adjustable parameters used to calculate the critical parameters of this mixture with high accuracy. The Δ_T and Δ_V values were determined on the basis of the present critical parameters of mixture listed in Table 3. The Δ_P value was determined taking into consideration the critical pressure of the R-32 + R-125 mixture by Nagel and Bier (1995) and Zhelezny et al. (1995). With respect to the R-32 + R-125 mixture, Δ_T, Δ_V, and Δ_P are −4.4 K, −15.81 cm^3/mol, and −0.05 MPa, respectively. The calculated values of the critical parameters for the R-32 + R-125 mixture are summarized in Table 4. The comparisons of the critical locus for the R-32 + R-125 mixture between the experimental data and the present correlation are shown in Figures 7−9. By using these adjustable parameters, the critical temperature of mixture can be calculated to be within ±0.1 K, whereas the critical molar volume can be reproduced to be within the experimental uncertainty. In addition, it was confirmed that the present critical parameter data of the R-32 + R-125 mixture were in good agreement with those by Nagel and Bier (1995), Bivens et al. (1995), and Zhelezny et al. (1995).

Acknowledgment

The authors are greatly indebted to Asahi Glass Co. Ltd., Tokyo, Japan, and Matsushita Electric Co. Ltd., Osaka, Japan, for kindly furnishing the samples and to Messrs. T. Ikeda, K. Kanai, M. Higuchi, H. Takashima, W. Sasanuma, K. Wakayama, J. Ohshima, K. Sakashita, and H. Nagamura, Iwaki Meisei University, for their valuable assistance in this experiment.

Literature Cited

Bivens, D. B.; Yokozeki, A.; Geller, V. Z. Thermodynamic Properties of R32/R125 Mixture. *Proc. 4th Asian Thermophys. Prop.* **1995**, *2*, 327−330.

Bouchot, C.; Richon, D. Simultaneous Measurements of Phase Equilibrium and Volumetric Properties by Vibrating Tube Densimetry: Apparatus and Results Involving HFC. *Proc. Int. Conf. "CFCs, The Day After"* **1994**, 517−524.

Boyes, S. J.; Weber, L. A. Vapour pressures and gas-phase (p, ρ_n, T) values for CF_3CHF_2(R125). *J. Chem. Thermodyn.* **1995**, *27*, 163−174.

Defibaugh, D. R.; Morrison, G.; Weber, L. A. Thermodynamic Properties of Difluoromethane. *J. Chem. Eng. Data* **1994**, *39*, 333−340.

De Vries, B. University of Hannover, private communication, 1996.

Fujiwara, K.; Momota, H.; Noguchi, M. Vapor-Liquid Equilibria of HFC-32 Mixture. *Proc.13th Jpn. Symp. Thermophys. Prop.* **1992**, 61−64.

Gorenflo, D.; Koester, R.; Herres, G. University of Paderborn, Germany, private communication, 1996.

Higashi, Y. Measurements of the Vapor-Liquid Coexistence Curve and the Critical Locus for Several Refrigerant Mixtures. *Int. J. Thermophys.* **1986**, *7*, 29−40.

Higashi, Y. Critical Parameters for HFC134a, HFC32 and HFC125. *Int. J. Refrig.* **1994**, *17*, 524−531.

Higashi, Y. Vapor-Liquid Equilibrium, Coexistence Curve and Critical Locus for Binary HFC-32/HFC-134a Mixture. *Int. J. Thermophys.* **1995**, *16*, 1175−1184.

Higashi, Y.; Uematsu, M.; Watanabe, K. Correlation of the Critical Curve for Binary Refrigerant Mixtures. *JSME Int. J.* **1988**, *31*, 573−580.

Holcomb, C. D.; Niesen, V. G.; Van Poolen, L. J.; Outcult, S. L. Coexisting Densities, Vapor Pressures and Critical Densities of Refrigerants R-32 and R-152a, at 300−385 K. *Fluid Phase Equilib.* **1993**, *91*, 145−157.

Kishizawa, G.; Sato, H.; Watanabe, K. Measurements of Saturation Densities in the Critical Region and Critical Loci for Binary R-32/125 and R-125/143a Systems. Presented at the 13th Symposium on Thermophysical Properties, Colorado, 1997.

Malbrunot, P. F.; Meunier, P. A.; Scatena, G. M.; Mears, W. H.; Murphy, K. P.; Sinka, J. V. Pressure−Volume Temperature Behavior of Difluoromethane. *J. Chem. Eng. Data* **1968**, *13*, 16−21.

Nagel, M.; Bier, K. Vapour-liquid Equilibrium of Ternary Mixtures of the Refrigerants R32, R125 and R134a. *Int. J. Refrig.* **1995**, *18*, 534−543.

Piao, C. C.; Thermodynamic Properties of HFC-32(Difluoromethane), submitted to *Int. J. Refrig.*, 1997.

Piao, C. C.; Noguchi, M. An Equation of State for Pentafluoroethane (HFC-125). *Fluid Phase Equilib.* **1996**, *125*, 45−54.

Polonara, F. University of Ancona, Italy, private communication, 1994.

Widiatmo, J. V.; Sato, H.; Watanabe, K. Saturated-liquid Densities and Bubble-point Pressures of the Binary Systems HFC-32 + HFC-125. *High Temp.−High Press.* **1993**, *25*, 677−683.

Widiatmo, J. V.; Sato, H.; Watanabe, K. Saturated-Liquid Densities and Vapor Pressures of 1,1,1-Trifluoroethane, Difluoroethane, and Pentafluoroethane. *J. Chem. Eng. Data* **1994**, *39*, 304−308.

Ye, F.; Sato, H.; Watanabe, K.; Gas-Phase PVT Properties and Vapor Pressures of Pentafluoroethane(HFC-125) Determined According to the Burnett Method. *J. Chem. Eng. Data* **1995**, *40*, 148−152.

Zhelezny, V.; Chernyak, Y.; Zhelezny, P. Critical Parameters for the Several Alternative Mixtures. *Proc. 4th Asian Thermophys. Prop.* **1995**, *2*, 291−294.

Received for review April 29, 1997. Accepted August 28, 1997.[⊗]

JE9701083

[⊗] Abstract published in *Advance ACS Abstracts,* October 1, 1997.